energies

Communication

Hybrid Nanofluid in a Direct Absorption Solar Collector: Magnetite vs. Carbon Nanotubes Compete for Thermal Performance

Pavel G. Struchalin [1,*,†], Dmitrii M. Kuzmenkov [2,†], Vladimir S. Yunin [2,†], Xinzhi Wang [3,†], Yurong He [3,†] and Boris V. Balakin [1,2,†]

1 Department of Mechanical and Marine Engineering, Western Norway University of Applied Sciences, Inndalsveien 28, 5063 Bergen, Norway; bbal@hvl.no
2 Institute of Nuclear Physics and Engineering, National Research Nuclear University "Moscow Engineering Physics Institute", Kashirskoe Highway 31, 115409 Moscow, Russia; dmkuzmenkov@mephi.ru (D.M.K.); vsyunin@mephi.ru (V.S.Y.)
3 Heilongjiang Key Laboratory of New Energy Storage Materials and Processes, School of Energy Science and Engineering, Harbin Institute of Technology, Harbin 150001, China; wangxz@hit.edu.cn (X.W.); rong@hit.edu.cn (Y.H.)
* Correspondence: pstr@hvl.no
† These authors contributed equally to this work.

Abstract: The paper presents the experimental measurements of thermal efficiency of a tubular direct absorption solar collector (DASC) with a hybrid nanofluid based on magnetite (Fe_3O_4) and multi-walled carbon nanotubes (MWCNT). The volumetric concentration of Fe_3O_4 and MWCNT was 0.0053% and 0.0045%, respectively. The experiments were carried out for the flow rates of 2–10 L/min and a temperature difference up to 20 °C between the environment and the DASC. The performance of the DASC with a hybrid nanofluid was in the range of 52.3–69.4%, which was just beyond the performance of the collector with surface absorption. It was also found that using a MWCNT-based nanofluid with an equivalent total volumetric concentration of particles (0.0091%), the efficiency was 8.3–31.5% higher than for the cases with the hybrid nanofluid.

Keywords: direct absorption solar collector; hybrid nanofluid; carbon nanotubes; magnetic nanofluid; iron oxide

check for updates

Citation: Struchalin, P.G.; Kuzmenkov, D.M.; Yunin, V.S.; Wang, X.; He, Y.; Balakin, B.V. Hybrid Nanofluid in a Direct Absorption Solar Collector: Magnetite vs. Carbon Nanotubes Compete for Thermal Performance. *Energies* **2022**, *15*, 1604. https://doi.org/10.3390/en15051604

Academic Editors: George Kosmadakis and Gianpiero Colangelo

Received: 28 January 2022
Accepted: 16 February 2022
Published: 22 February 2022

1. Introduction

Nanofluids (NFs) are stable solutions of nanosized particles dispersed in a carrier fluid [1]. With different and often superior thermal properties compared to a single-phase liquid [2–4], nanofluids improve the performance of thermal equipment [5], including solar collectors, both with surface absorption of solar radiation [6] and direct absorption solar collectors [7].

The direct absorption solar collector (DASC) with nanofluid is a perspective type of solar collector. An important feature of DASC is the volumetric absorption of solar radiation. It may result in a relatively cold outer surface and reduce thermal leaks.

Thermal efficiency is an important parameter of DASC. The parameter depends on the optical properties of the entire collector's absorber and used nanofluid. It is reported in the literature that nanofluids consisting of two or more types of particles (hybrid NF) absorb solar radiation in a wider spectral range than a single-particle-type nanofluid of the same particle concentration [8,9]. Therefore, the hybrid NFs are expected to influence the thermal efficiency of DASC. In addition, the use of hybrid NF with metal/metal oxide particles allows for applying magnetic fields in flow management [10].

Hybrid nanofluids have been sufficiently covered in the literature [11]. Many researchers claim the superiority of the hybrid nanofluid in the photothermal conversion process and potentially higher thermal performance in DASCs compared to the single-component nanofluid. However, there are a few systematic studies of hybrid NFs in a field-scale prototype DASC.

Mashhadian et al. [12] reported that Al_2O_3/MWCNT nanofluid increases the thermal efficiency of the direct absorption parabolic through collector (DAPTC) by 198%, 70%, and 6.1% compared to water, alumina nanofluids, and MWCNTs nanofluids of the same particle concentration. This result was not compared with the efficiency of a surface absorber of the same geometry. Menbary et al. [13] showed that thermal efficiency of DAPTC can achieve up to 48.03% when Al_2O_3/CuO NF is used. However, an evaluation of these results is challenging due to the lack of cases with single-component nanofluids and surface absorption of solar energy. Karami [14] reported that a flat-plate type direct absorption solar collector with single-component SiO_2 nanofluid had 28% lower thermal efficiency than with Fe_3O_4/SiO_2 hybrid nanofluid. Nevertheless, as in the studies above, the results were not compared with the efficiency of the surface energy absorption. Moreover, the experiments were done only at zero temperature drop between the liquid at the collector inlet and the environment.

In this work, we report the performance of a tubular DASC with Fe_3O_4/MWCNT nanofluid in different thermal regimes. We compare this data with cases of using MWCNT NF in DASC and surface absorption of solar energy.

2. Experiments

2.1. Nanofluid

The hybrid nanofluid was produced in several stages. Initially, two monocomponent nanofluids based on Fe_3O_4 and MWCNT were produced separately, sonicating commercial nanoparticles in a base fluid (water—10% wt. ethanol) for an hour. The ethanol was added to mimic field conditions where the heat transfer fluids are protected from a mild frost. Iron oxide particles (LLC "RSS Saransk", Saransk, Russia) had a maximum particle size of 110 nm in dry nanopowder (Figure 1). MWCNT (Nanotechnology Center, Saransk, Russia) had an inner diameter of 13.3 ± 0.45 nm and an external diameter of 49.3 ± 0.45 nm or 72.0 ± 0.45 nm (Figure 2). A rough estimate of maximum length is 5 µm. To stabilize the MWCNT nanofluid and to avoid foaming, we added 0.1% wt. sodium dodecyl sulfate (SDS) before and 0.4% wt. of defoamer "FoamStop" Kärcher after the sonication. Then, the monocomponent NFs were left for 24 h for gravitational separation. After that, the sedimented particles' agglomerates were removed and weighed, and the final concentration of particles in the nanofluid was calculated. Finally, the monocomponent NFs were mixed, and the concentrations of SDS and defoamer were restored to 0.1% wt. and 0.4% wt. The final volume fraction of the particles in hybrid NF was 0.0098%: it consisted of 0.0053% of Fe_3O_4 and 0.0045% of MWCNT.

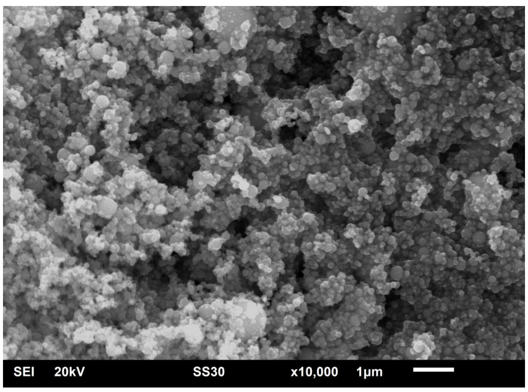

Figure 1. Microscopic images of iron oxide particles.

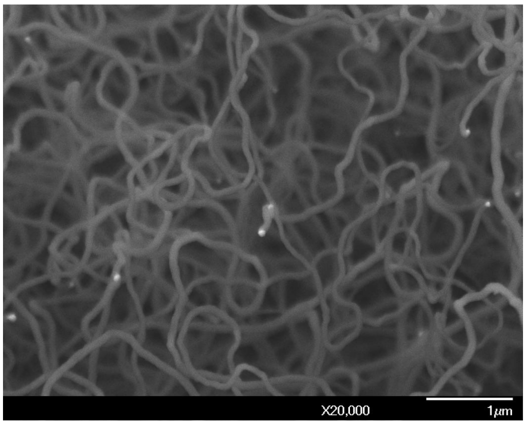

Figure 2. Microscopic images of multi-walled carbon nanotubes.

2.2. Experimental Set-Up

The nanofluid was tested in a lab-scale DASC (Figure 3) consisting of eight 1.5 m glass tubes (borosilicate glass 3.3 "SIMAX", ∅22 × 1.8 mm) connected in series. The tubes were irradiated by three halogen lamps (Osram Haloline Pro R7S, 400 W), which generated an average heat flux of I = 915 W/m^2 ± 10%. This value corresponds to a maximum solar heat flux available without concentration in Northern and Eastern Europe in summer [15]. The liquid was pumped by a centrifugal pump (Multi 14000E, Sicce) with a flow rate in a range of 2–10 L/min, which is typical for domestic solar heating systems [16]. The absorbed heat was removed from the liquid in the air heat exchanger coupled with a fan. The flow rate of nanofluid Q and its heating ΔT was measured by YF-S201 flowmeter from Foshan Shunde Zhongjiang Energy Saving Electronics Co., Ltd. (Foshan, China) (±10%) and T-type thermocouples (±0.08 °C). The temperatures of the ambient air and liquid in the expansion tank were measured by K-type thermocouples (±1 °C). The measurements were done in a steady thermal state at a constant flow rate. The liquid temperature was stabilized by changing the speed of the fan on the air heat exchanger and the flow rate through its bypass line. The air in the laboratory remained thermally stable during the entire process of the collector's stabilization and measurement. We started the measurements after about an hour from the moment of thermal stabilization of fluid in the tank. Further, all the temperatures and flow rates continued to be monitored and recorded for 15 min. Then, a new value of the flow rate in the collector was set, and another procedure of thermal stabilization was repeated. The measurements were done with the temperatures in the tank up to 20 °C higher than the environment temperature, which is consistent with the operating conditions of low-temperature solar collectors of domestic water heating systems [16].

The thermal efficiency of the collector η was given as (1) [17]:

$$\eta = \frac{\rho_l \cdot Q \cdot c_p \cdot \Delta T}{A \cdot I}, \quad (1)$$

where ρ_l, c_p are the density and specific heat of the liquid, respectively, and A is the irradiated area of the collector. Due to the low number of particles, the equivalent thermal properties of nanofluid were taken as for the base fluid [18–20]. It is consistent, for example, with the studies of Marcos et al. [21] and Wan et al. [22] of thermal properties of the dilute MWCNT-nanofluids. In the case of surface absorption of light, the glass tubes were covered by a black metal foil (reflection of 10%), and distilled water was pumped through the collector.

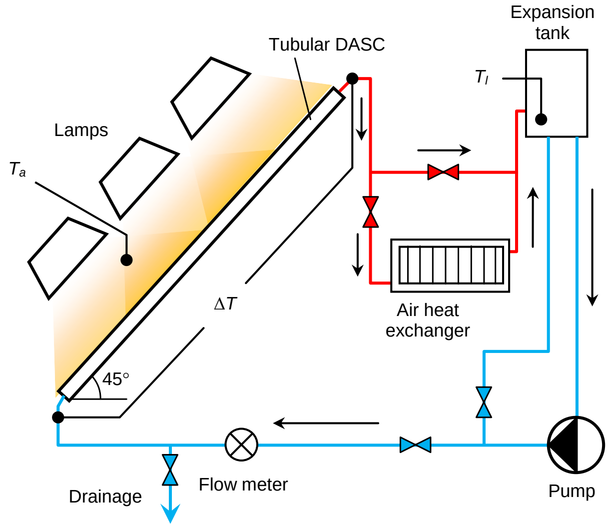

Figure 3. The experimental scheme.

3. Results and Discussion

Figure 4 integrates the results of the experiments in terms of the thermal efficiency of the DASC. In this figure, we present the combined uncertainties computed using a standard procedure available elsewhere (e.g., [17], Supplementary Materials). The uncertainties of the reference-based thermal properties of the liquid were not taken into account in this calculation. The primary source of the uncertainty of the thermal efficiency is the instrumental errors of the used measuring devices.

The efficiency of the collector is presented for four cases. The first basic case relates to the surface absorption of light. In the second case, water is pumped through the transparent tubes. The next cases relate to DASC with pumped hybrid and MWCNT nanofluids. The concentration of the MWCNT was 0.0091% vol., which was comparable to that of the hybrid nanofluid. From Figure 4, the collector efficiency with the hybrid nanofluid at $T_l - T_a = 10$ °C is lower by 6.7∼28.6% compared to the collector with surface absorption. The situation becomes slightly better at $T_l - T_a$ = 20 °C, where the hybrid nanofluid alters the collector's efficiency by −1.6∼+6.8% relative to the case with the opaque tubes. At the same time, when using MWCNT nanofluid, the collector efficiency increases by 2.7∼20.7% compared with the case of surface energy absorption. Thus, we conclude that using the Fe_3O_4/MWCNT hybrid nanofluid at a given concentration and ratio of particles is less effective than nanofluid with MWCNT particles.

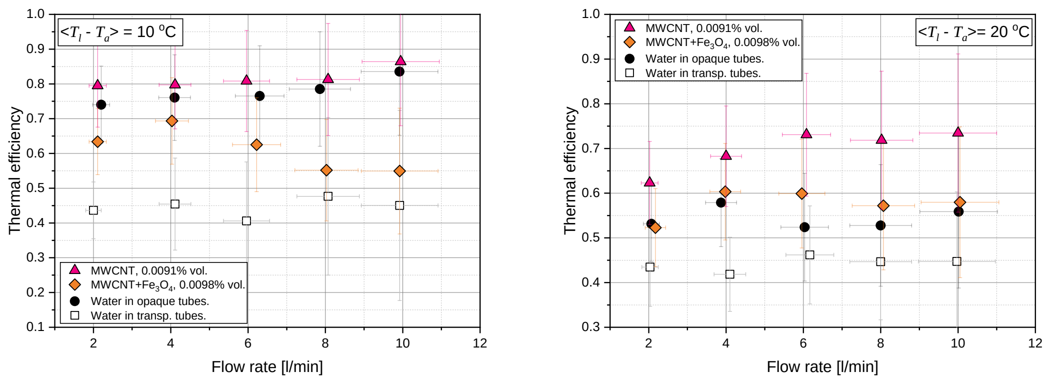

Figure 4. Efficiency of the tubular DASC for different flow rates, heat transfer fluids, and optical boundaries. The experiments are presented for Re = 2100∼11,000.

The obtained results can be explained by analyzing the optical properties of the nanofluids. Carbon nanotubes reduce the light radiation better than iron oxide nanoparticles ,resulting in a higher spectrum-averaged extinction coefficient for MWCNT nanofluid against Fe_3O_4/MWCNT hybrid nanofluid at a constant volumetric particle fraction. Furthermore, the shielding effect cannot be excluded when the carbon tube is partially or entirely “in the shadow” of iron oxide agglomerates. It further reduces light absorption in the nanofluid.

To evaluate the light-absorbing properties of hybrid Fe_3O_4/MWCNT nanofluid and single-particle MWCNT nanofluid, we measured the spectrum-averaged extinction coefficients of the considered nanofluids for two wavelength ranges: (R1) 400–1100 nm and (R2) 1000–1700 nm. As in our previous study [17], the extinction coefficients were determined by measuring the intensity reduction of a collimated light beam passing through the nanofluid. The extinction coefficients for the hybrid nanofluid were 199 m^{-1} for wavelength range (R1) and 380 m^{-1} (R2); and for the MWCNT nanofluid, the coefficients were 474 m^{-1}(R1) and 609 m^{-1}(R2). Thus, hybrid nanofluid has a lower extinction coefficient at an equivalent particle concentration and absorbs less thermal radiation than MWCNT nanofluid. This is consistent with the results reported by Tong et al. [23].

Figure 4 shows that the efficiency of the surface-absorbing collector decreases faster than that of the DASC when we increase the temperature difference with the environment. In this case, the volumetric absorption of solar energy by particles in the nanofluid reduces the temperature of the receiver, compared to the case with surface energy absorption. This limits the thermal leak to the environment for the nanofluid-based DASC.

From Figure 4, we further note the existence of an optimum flow rate at which the thermal efficiency is maximal. In our experiments, the optimum was about 6 L/min. The nanofluid becomes overheated at flow rates under the optimum due to longer exposure of nanoparticles. In this condition, the natural convection of air at the DASC surfaces intensifies and increases the thermal loss. Conversely, a higher flow rate intensifies forced convection from the nanofluid towards the DASC surface and increases the thermal leaks again [17]. However, the turbulent mixing of the nanofluid reduces the surface temperature at high flow rates and so levels up the negative influence of forced convection.

To provide estimates of convective heat transfer in the DASC, we calculated Nusselt numbers using Churchill’s expression for heat transfer in forced convection [24]. The results are presented in Table 1. They are supplemented with the calculations of the frictional pressure drop in the rig that are extracted from the recently-documented CFD model of our DASC [17].

As follows from the table, the DASC operates in a variety of flow regimes at Nu always greater than 4.3. Due to a number of bends, the pressure drop is about 1.7 kPa at the best-efficiency point and goes up to 4.0 kPa at the maximum flow rate.

Table 1. Nusselt numbers and pressure drops in the DASC.

Parameter	Range of the Values
Flow rate [L/min]	2 . . . 4 . . . 6 . . . 8 . . . 10
Re	2166 . . . 4333 . . . 6500 . . . 8667 . . . 10,834
Nu	4.5 . . . 31.7 . . . 61.8 . . . 78.1 . . . 93.9
Pressure drop [kPa]	0.4 . . . 0.9 . . . 1.7 . . . 2.6 . . . 4.0

Figure 5 compares the thermal efficiency of our DASC with the efficiency of the commercial solar collectors with surface energy absorption: flat-plate [25] and evacuated tubes types [26]. The nanofluid-based DASC demonstrates comparable efficiency with commercial models at low surface thermal resistances $(T_l - T_a)/I$. With increases in the temperature of the fluid, this advantage disappears. We explain it by a less than optimum thermal insulation of the top surface in the DASC and the lack of an anti-reflective coating.

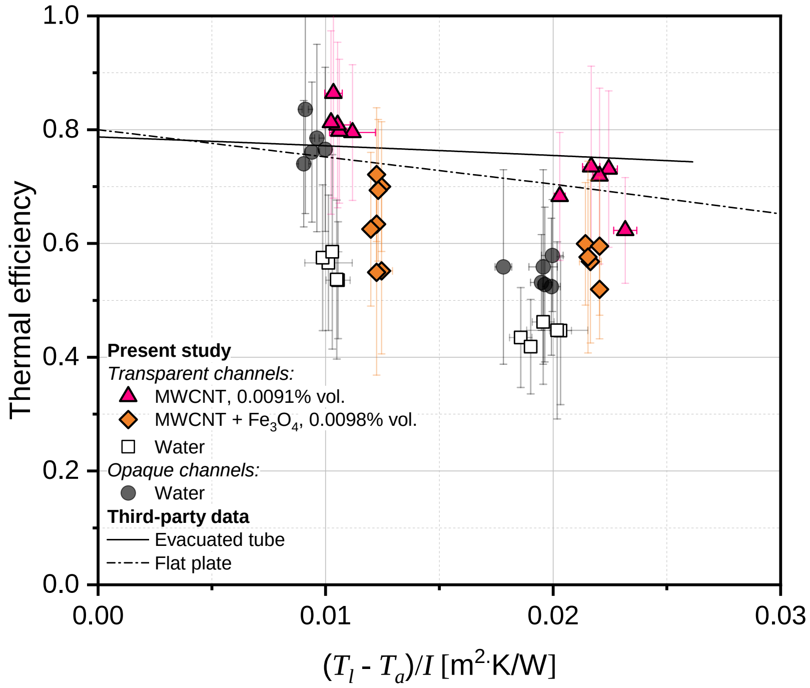

Figure 5. Thermal efficiency of a DASC with nanofluid and commercial collectors.

The particle deposition is a crucial point for the operation of the DASC. It can reduce the receiver transparency and, consequently, the volumetric absorption of light radiation in the fluid [27]. After the experiments, we visually inspected the inner surfaces of the DASC but did not detect the deposition of the particles. It is consistent with our previous study of MWCNT NF, where the local contamination of the loop began visibly at particle volume fractions above 0.0044% [17].

4. Conclusions

The present study revealed that the thermal efficiency of the tubular direct absorption collector with Fe_3O_4/MWCNT nanofluid was in the range of 52.3–69.4%. These values were just above the efficiency of the equally sized solar collector with surface absorption. At the same time, the DASC based on MWCNT nanofluid demonstrated higher thermal efficiency (62.3–86.4%) than the DASC with a hybrid nanofluid. This result is explained by the lower spectrum-averaged extinction coefficient of the hybrid nanofluid than the MWCNT nanofluid. However, we note that another composition of a hybrid nanofluid might result in a better optical performance. This is a subject of future research.

Author Contributions: Conceptualization, B.V.B.; methodology, P.G.S. and D.M.K.; formal analysis, X.W. and Y.H.; investigation, P.G.S., D.M.K. and V.S.Y.; data curation, P.G.S.; writing—original draft preparation, P.G.S., D.M.K., X.W. and Y.H.; writing—review and editing, B.V.B.; visualization, Y.H.; supervision, B.V.B. All authors have read and agreed to the published version of the manuscript.

Funding: Dmitrii M. Kuzmenkov and Xinzhi Wang thank RFBR and NSFC for support within research project No 20-58-53022.

Institutional Review Board Statement: Not applicable.

Informed Consent Statement: Not applicable.

Data Availability Statement: Not applicable.

Acknowledgments: We thank Nanotechnology Center, Russia, for providing microscopic images of MWCNTs.

Conflicts of Interest: The authors declare no conflict of interest. The funders had no role in the design of the study; in the collection, analyses, or interpretation of data; in the writing of the manuscript; or in the decision to publish the results.

References

1. Choi, S.S.; Eastman, A. Enhancing thermal conductivity of fluids with nanoparticles. *Dev. Appl. Non-Newton. Flows* **1995**, *231*, 99–105.
2. Boldoo, T.; Ham, J.; Cho, H. Comprehensive Experimental Study on the Thermophysical Characteristics of DI Water Based $Co_{0.5}Zn_{0.5}Fe_2O_4$ Nanofluid for Solar Thermal Harvesting. *Energies* **2020**, *13*, 6218. [CrossRef]
3. Kristiawan, B.; Rifa'i, A.I.; Enoki, K.; Wijayanta, A.T.; Miyazaki, T. Enhancing the thermal performance of TiO_2/water nanofluids flowing in a helical microfin tube. *Powder Technol.* **2020**, *376*, 254–262. [CrossRef]
4. Purnama, B.; Rahmawati, R.; Wijayanta, A.T.; Suharyana, S. Dependence of Structural and Magnetic Properties on Annealing Times in Co-precipitated Cobalt Ferrite Nanoparticles. *J. Magn.* **2020**, *20*, 207–210. [CrossRef]
5. Arshad, A.; Jabbal, M.; Yan, Y.; Reay, D. A review on graphene based nanofluids: Preparation, characterization and applications. *J. Mol. Liq.* **2019**, *279*, 444–484. [CrossRef]
6. Alam, T.; Balam, N.; Kulkarni, K.; Siddiqui, M.; Kapoor, N.; Meena, C.; Kumar, A.; Cozzolino, R. Performance Augmentation of the Flat Plate Solar Thermal Collector: A Review. *Energies* **2021**, *14*, 6203. [CrossRef]
7. Raj, P.; Subudhi, S. A review of studies using nanofluids in flat-plate and direct absorption solar collectors. *Renew. Sustain. Energy Rev.* **2018**, *84*, 54–74. [CrossRef]
8. Qu, J.; Zhang, R.; Wang, Z.; Wang, Q. Photo-thermal conversion properties of hybrid CuO-MWCNT/H_2O nanofluids for direct solar thermal energy harvest. *Appl. Therm. Eng.* **2019**, *147*, 390–398. [CrossRef]
9. Li, X.; Zeng, G.; Lei, X. The stability, optical properties and solar-thermal conversion performance of SiC-MWCNTs hybrid nanofluids for the direct absorption solar collector (DASC) application. *Sol. Energy Mater. Sol. Cells* **2020**, *206*, 110323. [CrossRef]
10. Alsaady, M.; Fu, R.; Yan, Y.; Liu, Z.; Wu, S.; Boukhanouf, R. An experimental investigation on the effect of ferrofluids on the efficiency of novel parabolic trough solar collector under laminar flow conditions. *Heat Transf. Eng.* **2019**, *40*, 753–761. [CrossRef]
11. Hu, G.; Ning, X.; Hussain, M.; Sajjad, U.; Sultan, M.; Muhammad Ali, H.; Shah, T.R.; Ahmad, H. Potential evaluation of hybrid nanofluids for solar thermal energy harvesting: A review of recent advances. *Sustain. Energy Technol. Assess.* **2021**, *48*, 101651. [CrossRef]
12. Mashhadian, A.; Heyhat, M.M.; Mahian, O. Improving environmental performance of a direct absorption parabolic trough collector by using hybrid nanofluids. *Energy Convers. Manag.* **2021**, *244*, 114450. [CrossRef]
13. Menbari, A.; Alemrajabi, A.A.; Rezaei, A. Experimental investigation of thermal performance for direct absorption solar parabolic trough collector (DASPTC) based on binary nanofluids. *Exp. Therm. Fluid Sci.* **2017**, *80*, 218–227. [CrossRef]
14. Karami, M. Experimental investigation of first and second laws in a direct absorption solar collector using hybrid Fe_3O_4/SiO_2 nanofluid. *J. Therm. Anal. Calorim.* **2019**, *136*, 661–671. [CrossRef]
15. Department of Geophysics, U.O.B. Været i Bergen (The Weather in Bergen). 2022. Available online: https://veret.gfi.uib.no/?action=period_query (accessed on 7 February 2022).
16. Popsueva, V.; Lopez, A.F.O.; Kosinska, A.; Nikolaev, O.; Balakin, B.V. Field Study on the Thermal Performance of Vacuum Tube Solar Collectors in the Climate Conditions of Western Norway. *Energies* **2021**, *14*, 2745. [CrossRef]
17. Struchalin, P.; Yunin, V.; Kutsenko, K.; Nikolaev, O.; Vologzhannikova, A.; Shevelyova, M.; Gorbacheva, O.; Balakin, B. Performance of a tubular direct absorption solar collector with a carbon-based nanofluid. *Int. J. Heat Mass Transf.* **2021**, *179*, 121717. [CrossRef]
18. National Institute of Standards and Technology. NIST Chemistry WebBook. Water. Available online: https://webbook.nist.gov/cgi/cbook.cgi?Name=water&Units=SI (accessed on 29 January 2021).
19. Stabnikov, V.N.; Royter, I.M.; Protsuk, T.B. *Ethanol*; Food Industry: Moscow, Russia, 1976. (In Russian)
20. Engineering ToolBox. Ethanol—Density and Specific Weight. 2018. Available online: https://www.engineeringtoolbox.com/ethanol-ethyl-alcohol-density-specific-weight-temperature-pressure-d_2028.html (accessed on 29 January 2021).
21. Marcos, M.A.; Podolsky, N.E.; Cabaleiro, D.; Lugo, L.; Zakharov, A.O.; Postnov, V.N.; Charykov, N.A.; Ageev, S.V.; Semenov, K.N. MWCNT in PEG-400 nanofluids for thermal applications: A chemical, physical and thermal approach. *J. Mol. Liq.* **2019**, *294*, 111616. [CrossRef]
22. Wan, M.; Yadav, R.R.; Mishra, G.; Singh, D.; Joshi, B. Temperature dependent heat transfer performance of multi-walled carbon nanotube based aqueous nanofluids at very low particle loadings. *Johns. Matthey Technol. Rev.* **2015**, *59*, 199–206. [CrossRef]
23. Tong, Y.; Boldoo, T.; Ham, J.; Cho, H. Improvement of photo-thermal energy conversion performance of MWCNT/Fe_3O_4 hybrid nanofluid compared to Fe_3O_4 nanofluid. *Energy* **2020**, *196*, 117086. [CrossRef]
24. Rohsenow, W.M.; Hartnett, J.P.; Cho, Y.I. *Handbook of Heat Transfer*; McGraw-Hill: New York, NY, USA, 1998; Volume 3.
25. NPOMASH. Flat-Plate Solar Collector SOKOL-EFFECT. Available online: http://www.sokolnpo.ru/ (accessed on 14 December 2020).

26. Viessmann Manufacturing Company. Vacuum Tube Solar Collector "Vitosol 200-T SP2A". Available online: https://www.viessmann-us.com/en/residential/solar/tube-collectors/vitosol_200-t_sp2a.html (accessed on 14 December 2020).
27. Sharaf, O.Z.; Al-Khateeb, A.N.; Kyritsis, D.C.; Abu-Nada, E. Four-way coupling of particle-wall and colloidal particle-particle interactions in direct absorption solar collectors. *Energy Convers. Manag.* **2019**, *195*, 7–20. [CrossRef]